Supplementary Information for

Polytype Family Representations of Octahedrally Coordinated Adaptive Structures in Ta_2O_5: Energetic and Dynamic Stabilities from First Principles

Dohyun Kim[1,2], Kun Hee Ye[1,2], Taeyoung Jeong[1,2], Seungjae Yoon[1,2], Yunjae Kim[1,2], Cheol Seong Hwang[*,2], and Jung-Hae Choi[*,1]

[1]*Electronic and Hybrid Materials Research Center, Korea Institute of Science and Technology, Seoul 02792, Korea*

[2]*Department of Materials Science and Engineering and Inter-University Semiconductor Research Center, Seoul National University, Seoul 08826, Korea*

**Corresponding author;*
Tel.: +82 2 880 7535. Fax: +82 2 884 1413
E-mail address: cheolsh@snu.ac.kr *(C. S. Hwang)*

Tel.: +82 2 958 5488. Fax: +82 2 958 6658
E-mail address: choijh@kist.re.kr *(J.-H. Choi)*

(a) alternating layer-normal directions

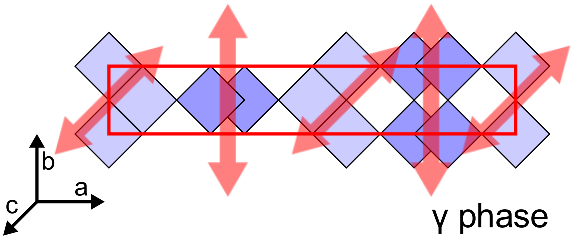

(b) corner-edge-sharing arrangements

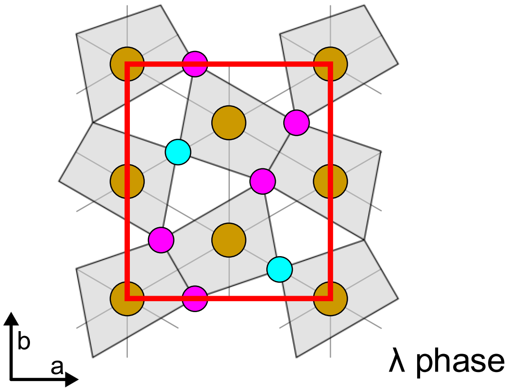

Fig S1 Allowed leniency on the two contexts of the adaptive structure. (a) The layered adaptive structure conventionally has Ta-O chains aligned in the same direction. To explain the γ phase with the layered adaptive context, it is allowed for each Ta ion to be able to define the layer-normal direction but not have to be aligned in the same direction. The red arrows indicate the alternating layer-normal directions. (b) The CS adaptive structure conventionally has two types of sharing between octahedra – corner- or edge-sharing. To explain the λ phase with the CS adaptive context, the 'corner-edge-sharing' should be allowed. Every intralayer 3-fold oxygen of the λ phase is the joint of corner-edge-sharing.

(a) P2/m phase

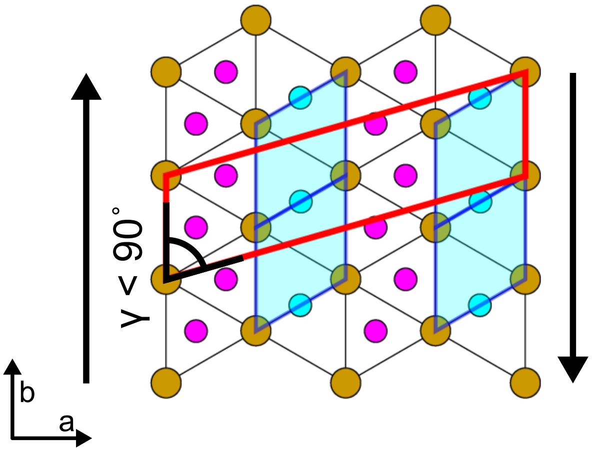

(b) Cmmm phase

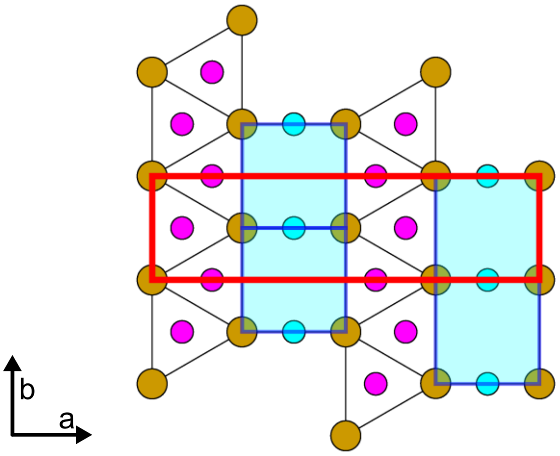

Fig. S2 Shear deformation between the two parallel phases of (a) P2/m and (b) Cmmm. To draw the occupation configuration of the Cmmm phase in the triangular Ta lattice, the symmetry should be reduced to P2/m. The γ angle may differ depending on the relaxation condition. The cyan-shaded '2-fold rhombus' is orthogonalized in the Cmmm symmetry.

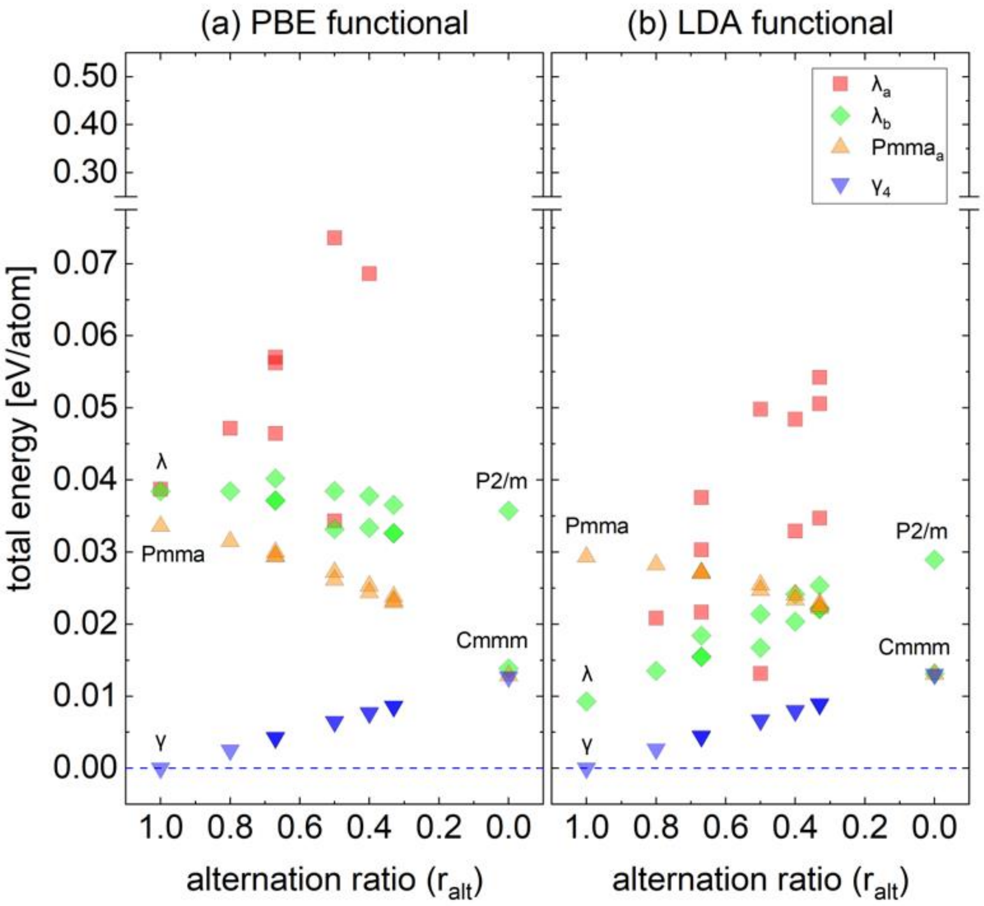

Fig. S3 Calculated energies of polytypic variants using (a) PBE functional and (b) LDA functional. Fig. 7(a) is replicated in (a) for ease of direct comparison. Within the LDA functional, the relative energies of the λ_a and λ_b polytype family are lowered, and the primary λ phase becomes energetically more stable than the primary Pmma phase.

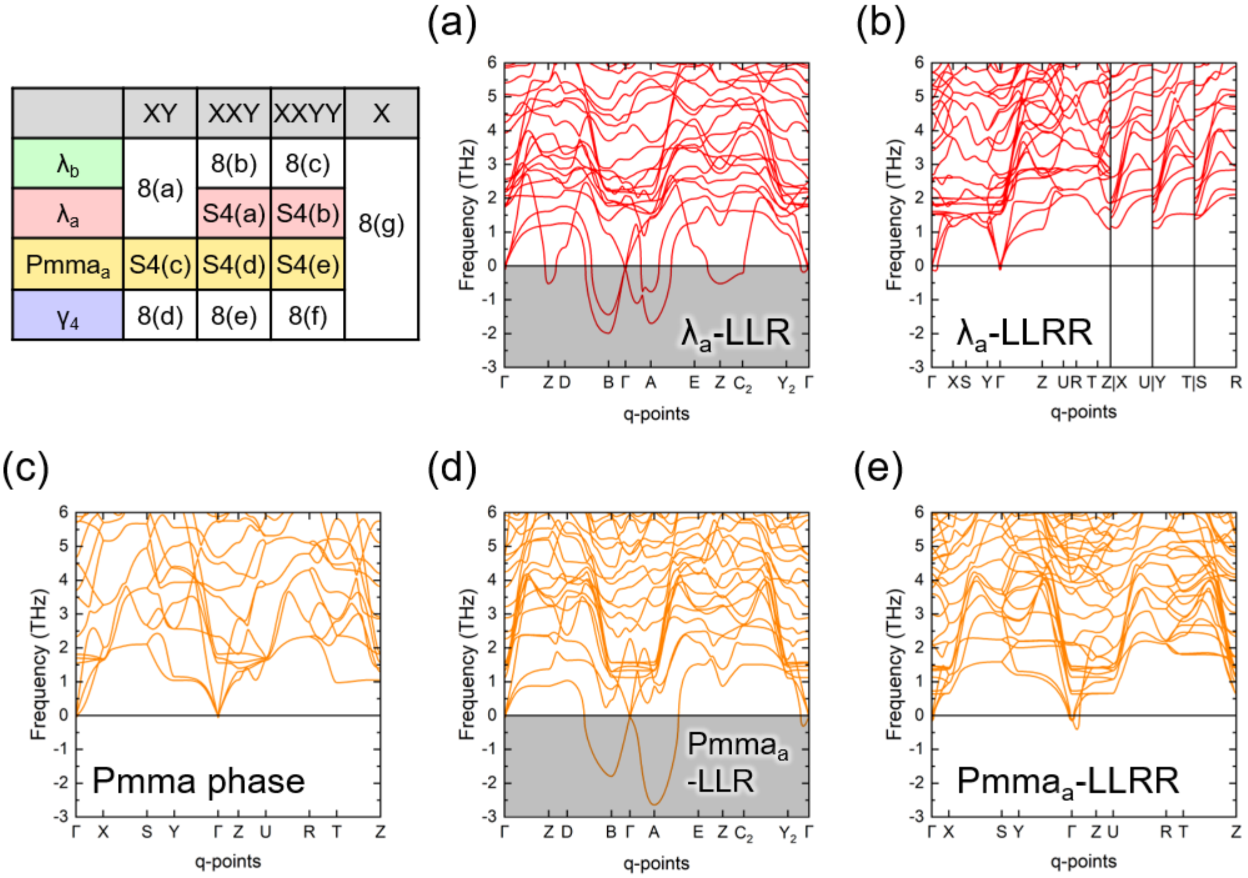

	XY	XXY	XXYY	X
λ_b	8(a)	8(b)	8(c)	8(g)
λ_a		S4(a)	S4(b)	
Pmma$_a$	S4(c)	S4(d)	S4(e)	
γ_4	8(d)	8(e)	8(f)	

Fig. S4. Phonon band diagrams of selected polytypic variants of λ_a and Pmma$_a$ polytype families in Fig. 6. The gray shade indicates a significant imaginary frequency. The indexing table briefly shows which figure each polytypic variant is located in.

Table S1. Ionic position of each polytype family. The positions are constructed in the schematic of the layered adaptive structure. The Ta lattice only consists of prisms of regular triangles and squares, and the ionic positions are snapped relative to this Ta lattice. The x, y, and z coordinates correspond to the height of the triangles, the side of the triangles, and the interlayer distances of the triangular prism, respectively. The relationship between x and y coordinates is illustrated below the table. The rows with element names indicate the positions of each ion in one structural unit (Ta_2O_5), with the next row showing the general position of the structural unit which should expand to a full plane, where n and m are arbitrary integers. The symmetry relations between the paired structural units (L-R and B-C) are listed below. Note that the glide-type polytype families have minus signs, and the screw-type polytype family has swapped y and z. The final 4 rows show how to stack the structural units, where X→Y denotes the transformation toward Y relative to X (Y=PX+Q). Every possible stacking sequence can be constructed with the operations listed.

Polytype family	λ_b			λ_a			$Pmma_a$			γ_4		
ionic position	x	y	z	x	y	z	x	y	z	x	y	z
Ta	0	0	0	0	0	0	0	0	0	0	0	0
Ta	1	1/2	0	0	1	0	0	1	0	1	1/2	0
$O_{3\text{-fold}}$	2/3	0	0	2/3	0	0	1/3	1/2	0	2/3	0	0
$O_{3\text{-fold}}$	1/3	1/2	0	1/3	1/2	0	-1/3	1/2	0	1/3	1/2	0
$O_{2\text{-fold}}$	3/2	1/4	0	1/2	5/4	0	1/2	5/4	0	5/3	1/2	0
$O_{\text{interlayer}}$	0	0	1/2	0	0	1/2	0	0	1/2	0	0	1/2
$O_{\text{interlayer}}$	1	1/2	1/2	0	1	1/2	0	1	1/2	1	1/2	1/2
full structural unit	+ (2n, 0, 1m)			+ (0, 2n, 1m)			+ (0, 2n, 1m)			+ (0, 1n, 1m)		
symmetry relation	L = (x, y, z) R = (-x, y, z)			L = (x, y, z) R = (x, -y, z)			L = (x, y, z) R = (x, -y, z)			C = (x, y, z) B = (x, z, y)		
L→L	(x, y+1, z)			(x+1, y-1/2, z)			(x+1, y-1/2, z)			(x+7/3, y+1/2, z)		
R→R	(x, y+1, z)			(x+1, y+1/2, z)			(x+1, y+1/2, z)			(x+7/3, y, z+1/2)		
L→R	(-x, y+1, z)			(x+1, -y-1/2, z)			(x+1, -y+1/2, z)			(x+7/3, z+1/2, y)		
R→L	(-x, y+1, z)			(x+1, -y+1/2, z)			(x+1, -y-1/2, z)			(x+7/3, z, y+1/2)		

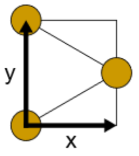

$$x = \frac{\sqrt{3}}{2} y$$

Table S2. Detailed explanation on the asterisked phases in Table 2, relaxed from the configuration of the λ_a polytype family. If the configuration is maintained or not changed significantly, the datapoints for those polytypic variants are shown in Fig. 7. Otherwise, the corresponding polytypic variant is not considered to be stable enough and is not shown in Fig. 7. The faulty relaxation of λ_a-LLLRRR into Pmma$_a$-LLLRRR has motivated the analysis of the Pmma phase. The faulty relaxation of λ_a-LLLLLR resulted in a theoretical polytype discussed in Fig. 4, which is beyond the scope of this study.

index in Table 2	r_{alt}	stacking sequence	space group after relaxation	structure after relaxation	datapoint shown in Fig. 7
#3	0.67	LLR	P2/m	Some broken 3-fold bonds	O
#8	0.4	LLLRR	P2/m	parallel P2/m phase	X
#9	0.4	LLLLR	Pm	broken 2-fold symmetry	O
#10	0.33	LLLRRR	Pmma	Pmma$_a$-LLLRRR	X
#11	0.33	LLLLRR	P2/m	parallel P2/m phase	X
#12	0.33	LLLLLR	Pm	mixture of Pmma$_a$ + λ_a	X (+0.056eV)

Supplementary Notes on the OD theory

The approach introduced in **section A** was inspired by the central principles of the order-disorder (OD) theory.[1-6] The OD theory systematically classifies the full symmetry of polytype structures by utilizing the partial symmetries – layer group of the polytype layers, and the relationships between adjacent polytype layers. A key requirement of this theory, known as the vicinity condition, specifies that every pair of adjacent polytype layers must be geometrically equivalent. The diversity of polytype structures arises from different stacking positions while maintaining the boundary structure unchanged. For example, the SiC polytypes, i.e., ABAB… for 2H (wurtzite) or ABCABC… for 3C (zinc blende), are based on the three possible positions of where the Si atoms can be located, in the close-packed structure manner.

In contrast, the polytypes considered in this study do not adhere to the vicinity condition, as the XY and XX pairs are not geometrically equivalent. In these cases, different partial symmetries (glide or screw vs. simple translation) between adjacent structural units differentiate the polytype structures. The approach of this work defines a polytype family based on structural units and the relationships between adjacent units, analogous to the OD theory. This demonstrates the applicability of the OD theory concept to more general cases of the polytypes.

Note that the SiC polytypes can be interpreted using the procedure of this study. From the 2H phase (space group $P6_3mc$, No. 186), the 6_3-screw operation divides the cell into two structural units with 180° rotated to each other. The notation directly corresponds to the Hägg notation,[7] where the [AB, BC, CA] and [BA, CB, AC] stackings are converted into $+$ and $-$, respectively. That is, the 2H phase (ABAB… = $+-+-$…) exhibits an alternating stacking sequence (primary phase), while the 3C phase (ABCA… = $++++$…) shows parallel stacking. These two phases are the maximum-degree-of-order (MDO) phases defined in the OD theory, which indicates a direct relationship between the approach of this paper and the OD theory.

References

1 K. Dornberger-Schiff, *Acta Crystallogr.*, 1956, **9**, 593-601.

2 K. Dornberger-Schiff and H. Grell-Niemann, *Acta Crystallogr.*, 1961, **14**, 167-177.

3 S. Ďurovič and Z. Weiss, *Bull. Minéral.*, 1986, **109**, 15-29.

4 B. Zvyagin, in *Crystal Symmetries*, Elsevier, 1988, pp. 569-591.

5 S. Ďurovič, P. Krishna and D. Pandey, *International Tables for Crystallography*, 2006, **C**, 752-773.

6 S. Merlino, *Z. Kristallogr. Krist.*, 2009, **224**, 251-260.

7 G. Hägg, *Ark. Kemi. Miner. Geol.*, 1943, **16B**, 1-6.